SHORT COMMUNICATION

Microstructure and properties of $AlTiNiMnB_x$ high entropy alloys

C. Li, J. C. Li*, M. Zhao, L. Zhang and Q. Jiang

$AlTiNiMnB_x$ (x=0·1, 0·2, 0·4 and 0·5) high entropy alloys are prepared by an arc furnace. The results show that the alloys have a single bcc crystal structure. Boron additions lead to distortion of the crystal lattice and alloy strengthening. The highest hardness (779 HV) is achieved with 0·5 at.-%B.

Keywords: High entropy alloys, Microstructure, Properties

Introduction

Usually, alloy systems have been based mainly on one principal element as a matrix, such as iron, copper, aluminium, magnesium, titanium, etc. Many researchers have explored a wide range of bulk amorphous alloys where the concept of multicomponents is taken to drop the melting temperature and to increase the difficulty of crystallisation.[1–7] However, one essential component of the alloys is usually more than 50%. It is known that when solubility is high, the solid solution based on one principal element can increase the strength of the solution due to the solution hardening. As the amount of alloying element increases, intermetallic compounds are typically formed in the alloy due to limited solid solubility, and this leads to increased strength, but at the expense of accompanying embrittlement. If the formation of intermetallic compounds were avoided where the alloy has a single crystal lattice, the alloy would have a better combination of strength and plastics. Based on the thermodynamic principle, a new alloy design concept, 'multiprinciple element alloy', was explored by Yeh *et al.*, which was named as high entropy (HE) alloy and consists of simple fcc or bcc solid solution phases.[8–10] High entropy alloys as multi component alloys are composed of n major alloy elements with $n \geqslant 5$ in equimolar or near equimolar ratios. This leads to an increase in stability of the solution due to the maximising the mixing entropy. Following Boltzmann's hypothesis on the relationship between entropy complexity,[8] the configurational entropy change per mole ΔS_{conf}, during the formation of a solid solution from n elements with equimolar fractions, may be calculated from the following equation.

$$\Delta S_{\text{conf}} = -R\left[\frac{1}{n}\ln\left(\frac{1}{n}\right)+\frac{1}{n}\ln\left(\frac{1}{n}\right)+\ldots+\frac{1}{n}\ln\left(\frac{1}{n}\right)\right]$$
$$= -R\ln\left(\frac{1}{n}\right) = R\ln(n) \quad (1)$$

where R is the gas constant. When n=5, ΔS_{conf}=1·61R, which approaches the size of the melting entropy of most intermetallic compounds (about R–2R). As results, intermetallic compounds are absent and a single solid solution is built with structures of a single fcc, a single bcc or fcc + bcc.[8–10] Owing to the above structural and compositional characteristics, the HE alloys are ductile, work hardenable, and strong at high temperature up to 800°C.[11–13] Thus, the alloys have potential applications as high temperature structure materials and work tools.

To further improve the hardness of the alloys, in this contribution, boron element, which usually is a valid alloying element to increase the materials hardness, is added to the alloys. After the fabrication of the alloy by an arc furnace melting, the microstructure and the mechanical properties of the alloys are measured and the effects of alloying element boron on the structure and properties are discussed.

Experimental

The $AlTiNiMnB_x$ HE alloys are prepared by a vacuum furnace under argon atmosphere. The rod and slice shaping ingot of the alloy are obtained in a cold copper hearth with a cooling rate of $\sim 10^4$ K s^{-1}. The diameter of rod is 6 mm while the slice thickness is 1 mm. Table 1 shows the composition of the alloys. The phase structure analysis of the samples was made by Rigaku D/max. 2500 X-ray diffractometer at 50 kV and 250 mA. Scanning angles ranged from 25 to 135° with a scanning rate of 5° min^{-1}. The microstructure of the alloys was observed using optical microscope (OP). The hardness of the samples was determined by a Vickers hardness instrument. Vickers' load was 200 g with a loading time of 15 s. The density was determined by use of Archimedes' principle by a balance with a precision of 0·01 mg.

Table 1 Composition of alloys used in experiment

Alloy no.	Al	Ti	Ni	Mn	B	Atomic ratio
1	24·4	24·4	24·4	24·4	2·4	$AlTiNiMnB_{0·1}$
2	23·8	23·8	23·8	23·8	4·7	$AlTiNiMnB_{0·2}$
3	22·7	22·7	22·7	22·7	9·1	$AlTiNiMnB_{0·4}$
4	22·2	22·2	22·2	22·2	11·1	$AlTiNiMnB_{0·5}$

The Key Laboratory of Automobile Materials of Ministry of Education and Department of Materials Science and Engineering, Jilin University, Changchun 130025, China

*Corresponding author, email ljc@jlu.edu.cn

Published by Maney on behalf of the Institute
Received 21 September 2007; accepted 12 November 2007
DOI 10.1179/174328408X275964

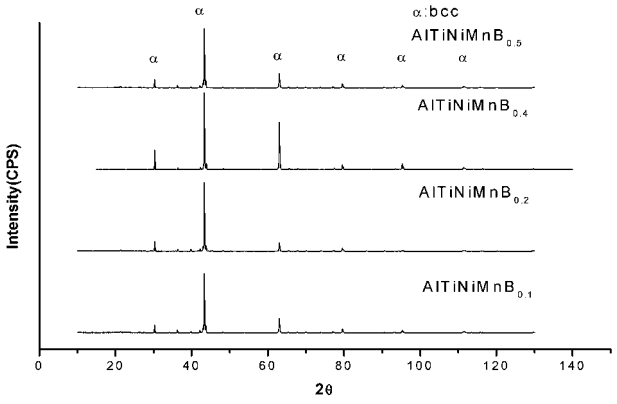

1 X-ray diffraction curve analysis of alloys with different boron contents

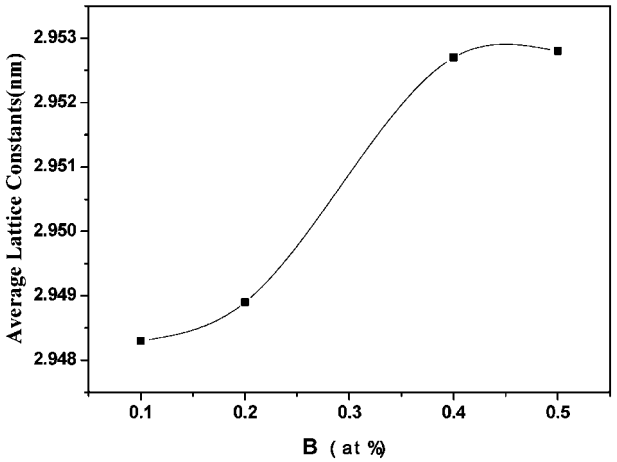

2 Lattice constants of alloys with different boron contents

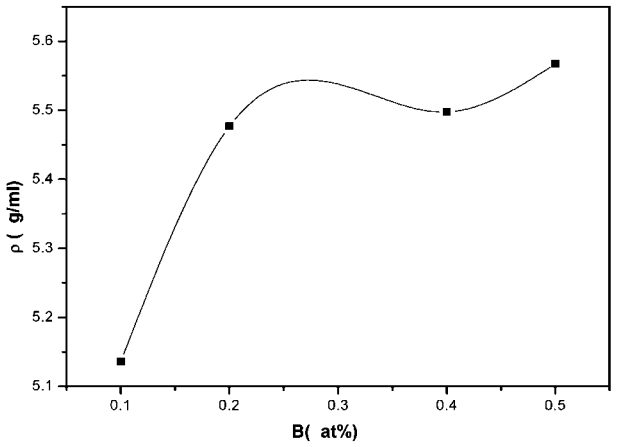

3 Density of alloys with different boron contents

Results and discussion

The alloys contain different kinds of elements with different amount where the composition of alloys has an equimolar ratio except the element boron. X-ray phase analysis results of the alloys with different boron contents are shown in Fig. 1. The alloys consist of a single ordered bcc phase. The intensity of the diffraction peak decreases with increasing boron content because addition of boron element induces aberrance of the crystal lattice.

Figures 2 and 3 show that the lattice constant and the density of the alloys increase with increasing boron content. The former increases from 2·9483 to 2·9528 nm, and latter from 5·14 to 5·57 g mm^{-3}. Since the atomic radius of boron is smaller than other alloying elements in the alloys, boron locates at interstitial, but

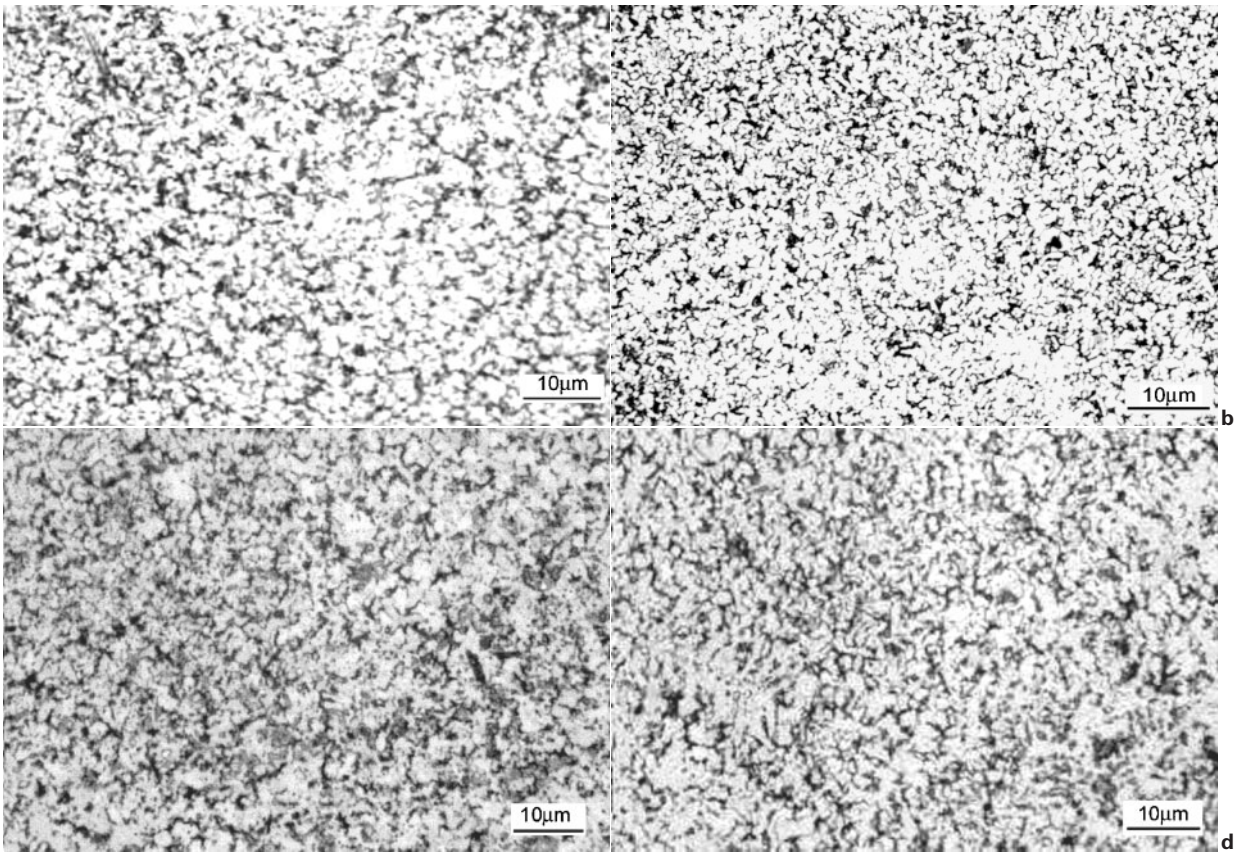

a $AlTiNiMnB_{0·1}$ alloy; *b* $AlTiNiMnB_{0·2}$ alloy; *c*$AlTiNiMnB_{0·4}$ alloy; *d* $AlTiNiMnB_{0·5}$ alloy

4 Optical micrographs of alloys with different boron contents

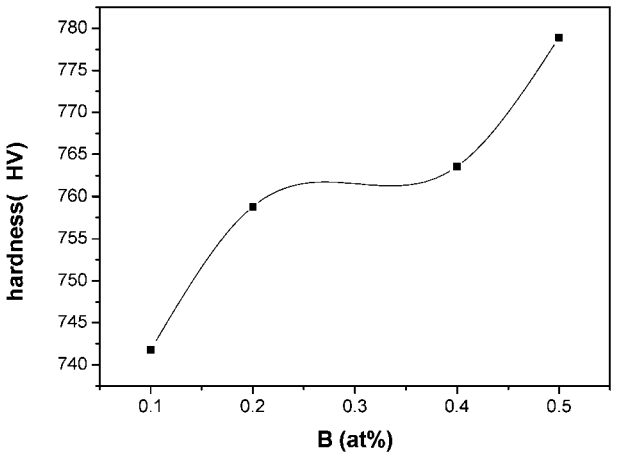

5 Vickers hardness of $AlTiNiMnB_x$ alloys with different boron contents

not substitutional position in the bcc solution. This characteristic leads to the formation of a single solid solution without appearance of borides. As results, the lattice constant and the density increase.

Boron content not only induces the lattice strain, but also affects the micorstructure and the properties of the alloys. Figure 4 presents the microstructure of the alloys with distinct boron contents. The results show that the microstructure is a typical dendritic crystal structure in a casting state. The microstructure of the alloys becomes finer with increasing boron content. While boron content is more than 0·5%, the brittleness of the alloys is enhanced.

Figure 5 gives the hardness of alloys as a function of the boron content. The result shows that the alloys possess high hardness. The hardness increases from 740 to 779 HV as boron content increases, which could be induced by the aberrance of crystal lattice.

Summary

$AlTiNiMnB_x$ HE alloys with different boron contents exhibit a single bcc solid solution phase. The crystal lattice constant and the density of the alloys increase with increasing boron content, which results in a significant increase in hardness. The highest hardness of the alloys reaches ~780 HV.

Acknowledgement

The financial supports from NNSFC (grant no. 50571040) and 985 Project of Jilin University are acknowledged.

References

1. A. Takeuchi and A. Inoue: *Mater. Trans. JIM*, 2000, **41**, 1372–1378.
2. A. Inoue, K. Ohtera, K. Kita and T. Masumoto: *Jpn J. Appl. Phys.*, 1988, **27**, L2248–L2251.
3. H. W. Kui, A. L. Greer and D. Turnbull: *Appl. Phys. Lett.*, 1984, **45**, 615–616.
4. A. Inoue, T. Zhang and T. Masumoto: *Mater. Trans. JIM*, 1990, **31**, 177–183.
5. A. Peker and W. L. Johnson: *Appl. Phys. Lett.*, 1993, **63**, 2342–2344.
6. R. Akatsuka, T. Zhang, M. Koshiba and A. Inoue: *Mater. Trans. JIM*, 1999, **40**, 58–261.
7. T. Zhang and A. Inoue: *Mater. Trans. JIM*, 1998, **39**, 857–862.
8. J. W. Yeh, S. K. Chen, S. J. Lin, J. Y. Gan, T. S. Chin, T. T. Shun, C. H. Tsau and S. Y. Chang: *Adv. Eng. Mater.*, 2004, **6**, 299–303.
9. J. W. Yeh, S. K. Chen, J. Y. Gan, S. J. Lin, T. S. Chin, T. T. Shun, C. H. Tsau and S. Y. Chang: *Metall. Mater. Trans. A*, 2004, **35A**, 2533–2536.
10. P. K. Huang, J. W. Yeh, T. T. Shun, S. K. Chen: *Adv. Eng. Mater.*, 2004, **6**, 74–78.
11. C. Y. Hsu, J. W. Yeh, S. K. Chen and T. T. Shun: *Metall. Mater. Trans. A*, 2004, **35A**, 1465–1469.
12. Y. Y. Chen, T. Duval, U. D. Hung, J. W. Yeh and H. C. Shih: *Corros. Sci.*, 2005, **47**, 2257–2279.
13. C. Y. Hsu, J. W. Yeh, S. K. Chen, T. T. Shun: *Metall. Mater. Trans. A*, 2004, **25A**, 1465–1469.